

# Molecular scale simulation of hole mobility and current densities in amorphous tridecane

Mikael Unge and Christer Törnkvist  
 ABB Corporate Research  
 Västerås, Sweden  
 mikael.unge@se.abb.com

Pascal Kordt and Denis Andrienko  
 Max Planck Institute for Polymer Research  
 Mainz, Germany

**Abstract**—The hole mobility of amorphous tridecane (a model of amorphous polyethylene) is simulated using a parameter-free approach which combines density functional theory, molecular dynamics and kinetic Monte Carlo methods. We observe large variations of the current density in the samples, typical to materials with large energetic disorder. The obtained mobility values are of the same order of magnitude as the highest experimentally reported values. By introducing carbonyl groups, we assess the effect of material oxidation and find that the mobility is reduced by an order of magnitude already at moderate concentrations of these groups.

**Keywords**—Hole mobility, simulation, tridecane, polyethylene

## I. INTRODUCTION

The performance of dielectrics, determined by their breakdown strength, dielectric loss, and conductivity, strongly depends on the underlying chemical composition, morphology, and post-processing of the material [1-3]. For polymeric insulators, such as polyethylene (PE) and cross-linked PE (XLPE), the cross-linking by-products [4, 5] and oxidation [3, 6] are known to affect the conductivity. Phenomenological effective models are often employed to understand observed phenomena [7-9]. They, however, require experimental input in order to deduce model parameters and do not provide a direct link to the chemical composition, making it difficult to design new compounds.

On a molecular scale, diffusion of molecules/ions and electron/hole traps has been used to explain experimental data. These explanations can be assisted by parameter-free modeling, such as density functional theory (DFT) calculations, which can be used to determine the trap depth of different dielectrics, in particular in PE and oxidized PE [10-12]. On the atomic level, a link between the semi-crystalline structure of PE [13-15] and its conductive properties can be elucidated by means of molecular dynamics (MD) simulations, capable of generating geometries of solid dielectrics [14, 15]. There are also a few studies on the charge dynamics (mobility) of electrons and holes in these dielectrics [14, 16-18].

In this paper we use a computational approach, initially developed to study charge transport in organic semiconductors, in order to evaluate conductivity of

dielectrics. In a nutshell, MD is used to simulate amorphous material morphologies, DFT and polarizable force-fields to evaluate charge transfer rates, and kinetic Monte Carlo (KMC) to perform charge transport simulations. The charge mobility is therefore obtained without any *a priori* assumptions about the system.

A comprehensive model of the PE morphology is challenging: PE shows crystalline regions and segregation as well as amorphous regions. Effects like chain folding make the morphology very sensitive to the temperature and to the production procedure. The morphological properties have been an important topic for over 50 years and are beyond the scope of this work [19]. Here we therefore limit our investigation to the amorphous phase which is modeled by an amorphous phase of n-tridecane (TRI). TRI has previously been used in experiments as a model of PE [20]. In particular, we investigate the hole mobility and current density and how it is affected by oxidation. Effects of oxidation are modeled by introducing a certain percentage of carbonyl groups into TRI molecules.

It has been suggested that holes are the dominating charge carriers in PE at low fields [21, 22], which is why we limit our investigations to hole transport. Our model system (tridecane instead of PE) obviously lacks the contribution to the mobility due to transport along polymer chains. Hence, it provides the lower bound for charge mobility, taking into account only inter-chain charge transport.

Experimental investigations report a charge density in the order of  $10^{15}$ - $10^{16}$  m<sup>-3</sup> at fields below 5 kV/mm [23] and  $10^{18}$ - $10^{19}$  m<sup>-3</sup> at fields 15-20 kV/mm [8] in low density PE (LDPE). Due to these low values we can neglect effects of carrier interaction in our charge transport simulations. Reported mobility values in LDPE differ depending on experimental method and field. Typical values are in the order of  $10^{-15}$ - $10^{-9}$  m<sup>2</sup>/Vs [8, 24, 25]. The wide range of values of reported charge densities and mobilities indicates the complexity of the problem and motivates our simulation study of hole mobility in solid dielectrics.

## II. METHODOLOGY

The key points of the methodology used in this work are described in this section. A detailed description can be found in [26, 27].

### A. Morphology

The initial guess of the amorphous morphology is obtained by using the ‘‘Amorphous Builder’’ of *Materials Studio*, which uses a Monte Carlo based technique to pack the molecules at a given density, here set to  $0.9 \text{ g/cm}^3$  [28]. We use a quadratic box of 512 molecules with 5.8 nm side length in the final configuration. The geometries are then optimized and relaxed using MD and the COMPASS force field in *Materials Studio*. The initial energy minimization stage is carried out using the Conjugate Gradient method. Finally, the structure is relaxed with MD simulations in the *NVT* ensemble at 298 K, and then in the *NVE* ensemble for about 5 ps. The final densities are around  $0.85 \text{ g/cm}^3$ , which is higher than reported experimental values for TRI, but is close to the density of the amorphous phase of PE,  $0.86 \text{ g/cm}^3$ . The obtained structures are used to study hole transport as summarized in the next section.

### B. Charge Transfer

In amorphous organic semiconductors and insulators electronic states are localized on a single molecule. This allows to use the non-adiabatic approximation for charge transfer, where the electronic coupling between two diabatic states is small and the molecular rearrangement after a charge transfer, described by the reorganization energy,  $\lambda_{ij}$ , plays an important role. Here we use the ‘‘high-temperature’’ limit of the charge transfer theory which neglects tunneling effects at very low temperatures. The charge transfer rate in this limit is given by the Marcus rate expression [29, 30]

$$\omega_{ij} = \frac{2\pi}{\hbar} \frac{J_{ij}^2}{\sqrt{4\pi\lambda_{ij}k_{\text{B}}T}} \exp\left[-\frac{(\Delta\varepsilon_{ij}-\lambda_{ij})^2}{4\pi\lambda_{ij}k_{\text{B}}T}\right] \quad (1)$$

where  $T$  is the temperature,  $J_{ij}$  is the transfer integral,  $\lambda_{ij}$  is the reorganization energy and  $\Delta\varepsilon_{ij}$  is the site energy difference. All molecules closer to each other than 0.5 nm are added to a neighbor list. Charge transfer can occur for all molecules in this list, for which charge transfer rates are evaluated. The electronic coupling,  $J_{ij}$ , between two localized states is calculated using DFT in NWChem [31] using the PBE functional, the 6-31G basis set, and the dimer projection method [32].

The site energies entering the Marcus rate are calculated using the expression

$$\varepsilon_i = \varepsilon_i^{\text{int}} + \varepsilon_i^{\text{el}} + q\mathbf{E} \cdot \mathbf{r}_i. \quad (2)$$

Here  $\varepsilon_i^{\text{int}}$  is the ionization potential of the molecule, evaluated by a DFT calculation (PBE-631G) in the gas phase.  $\varepsilon_i^{\text{el}}$  is the electrostatic energy, evaluated using Coulomb interaction of partial charges with a maximal interaction length of 3 nm. The last term describes the effect of an external electric field,  $\mathbf{E}$ .

The reorganization energy,  $\lambda_{ij}$ , is the change in the energy of a system due to its geometric relaxation upon charging or discharging. Here we neglect the ‘‘outersphere’’ contribution to the reorganization energy which is due to relaxation of the environment. The intramolecular contribution is evaluated in a gas-phase using DFT from four molecular states.

### C. Charge Mobility

Charge transport is described by the Master equation. We solve it using a KMC algorithm [27] with periodic boundary conditions. A single charge carrier is used in the KMC simulations, which is justified by the low charge concentration in the investigated systems. The hole mobility,  $\mu$ , is calculated directly from the KMC trajectory as  $\mu = x/Et$ , where  $x$  is the travelled distance in the field direction,  $E$  is the absolute value of the field and  $t$  the simulated time. The simulation is stopped after  $10^8$ - $10^{10}$  steps depending on the energetic disorder in the system. Mobilities are averaged over 50 runs each. In small systems with low carrier density and high energetic disorder one faces the problem of artificially increased mobilities at room temperature. We therefore apply an extrapolation procedure [33], that consists of simulations at increased temperatures, fitting to a mobility–temperature relation, and subsequent extrapolation down to room temperature.

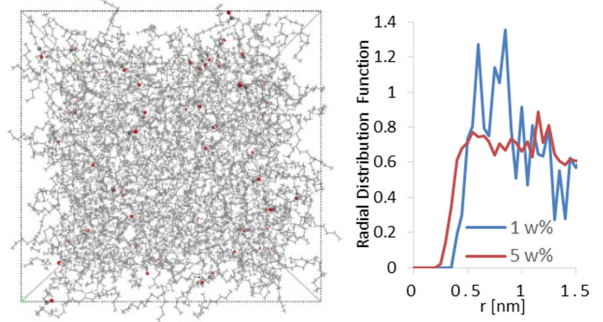


Fig. 1. Left: System of TRI with 1 w% carbonyl groups. Right: Radial distribution function of oxygen content of the 1 w% and 5 w% system, respectively.

## III. RESULTS

We study pure TRI as well as several systems with varying content of carbonyl groups. Carbonyl groups have been identified as the origin of deep energetic traps for both electrons and holes in several computational studies. Hence, it is expected that at a low carbonyl concentration charges are trapped at the carbonyl groups. At higher concentrations, however, direct hopping between carbonyl groups is possible due to a decreased distance and an increased charge transfer between the carbonyl sites.

### A. Geometries

Fig. 1 shows an exemplary geometry of amorphous TRI with 1 w% of carbonyl groups. The concentration values are calculated as the fraction of the atomic mass of one carbon and one oxygen atom to the total number of atoms. Since the transfer integral between two sites is distance dependent, it is

of interest to analyze the average distance between carbonyl groups. This is done by calculating the radial distribution function (RDF) of the oxygen atoms. For 0.1 w% the distance is large, in the order of 1 nm. In Fig. 1 RDFs of the 1 w% and 5 w% systems are shown. The shortest distances between oxygen atoms are around 4.5 Å in the 1 w% system and 3.0 Å in the 5 w% system. Transfer integrals for the systems are shown in Fig. 2. For the 0.1 and 1 w% system there is a reduction in the lower values compared to the pure TRI system. At 5 w% the mean value of the transfer integrals is significantly shifted downwards. To gain an understanding of this effect, the inset in Fig. 2 shows the highest occupied molecular orbitals (HOMO) of oxidized TRI (oTRI) and TRI. The HOMO of oTRI is localized on the carbonyl group while the HOMO of TRI is delocalized over the entire molecule. This, of course, leads to different conditions for the HOMO overlap. An improved model would include a random positioning of the carbonyl groups on the molecule instead of the approach here where all oTRI are the same and the carbonyl is positioned in the middle of the molecule.

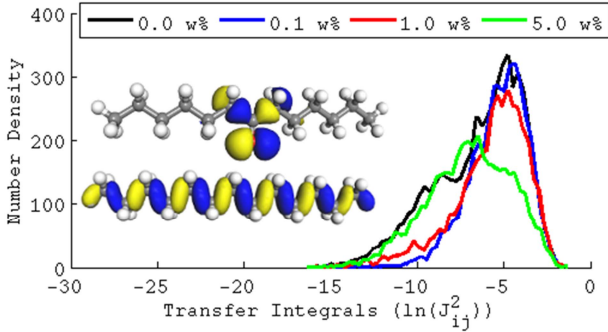


Fig. 2. Histogram of calculated transfer integrals for different carbonyl-group concentrations. Inset: HOMO of TRI with carbonyl group (top) and TRI (bottom), respectively.

Fig. 3 shows site energy distributions for different carbonyl concentrations. Between the pure TRI system and the system with the lowest carbonyl concentration there is only a small difference. At higher concentration the distributions widen, clearly showing deep traps of carbonyl groups. The hole trap level for carbonyl in PE is calculated to be around 0.8 eV [11, 12]. At 5 w% the standard deviation decreases even more as compared to the 1 w% case, since now the majority of molecules is oTRI (377 out of 512). Hence, for the 1 and 5 w% system one can expect a significant reduction of the mobility due to the large energetic disorder.

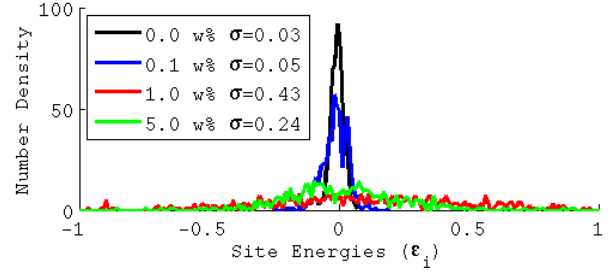


Fig. 3. Distribution of site energies in the different systems.

### B. Charge dynamics

The simulation of hole mobility was performed using KMC and electric fields in the range of 1-100 kV/mm. The pure TRI system shows a weak field dependence and values of the mobility of  $1.7 \times 10^{-6} \text{ m}^2/\text{Vs}$ . For the 0.1 w% system the mobility values are in the range of  $10^{-7}$ - $10^{-6} \text{ m}^2/\text{Vs}$ . The mobility decreases to  $\sim 10^{-14} \text{ m}^2/\text{Vs}$  for the 1 w% system. At 5 w% the mobility becomes extremely low,  $\sim 10^{-35} \text{ m}^2/\text{Vs}$ , indicating that the charge transport in dielectric liquids with trap densities at this level is mainly governed by ionic conduction. In a polymer the mobility could be higher due to transport along the polymer backbone.

We should also note that small simulation systems may lead to artificially increased mobility values [33]. To account for finite-size effects, mobility simulations are performed at elevated temperatures, where the mobility is not affected by the size of the simulation box. The temperature threshold,  $T_{\text{ND}}$ , where this is the case is obtained from the relation  $(\sigma/k_B T_{\text{ND}})^2 = -5.7 + 1.05 \ln N$ , where  $\sigma$  is the standard deviation of site energies and  $N$  the number of molecules. The values for  $T_{\text{ND}}$  for the systems are 350, 750, 10000 and 5500 K for 0.0, 0.1, 1.0 and 5.0 w%, respectively. Simulations are performed above these temperatures up to 50000-75000 K. The structure is kept fix at its room temperature configuration. The obtained values are used to extrapolate to room temperature mobility of  $1.7 \times 10^{-8} \text{ m}^2/\text{Vs}$  and  $1.8 \times 10^{-9} \text{ m}^2/\text{Vs}$  for the 0.0 w% and 0.1 w% systems, respectively, at 10 kV/mm. In Fig. 4 the scaled mobility at room temperature (298 K) is shown as function of the applied field for the pure TRI and with 0.1 w% CO, respectively. The almost constant mobility for the pure TRI system could be a result of the low energetic disorder in the system. With 0.1 w% of CO a clear Poole-Frenkel field dependence,  $\mu = \mu_0 \exp(\alpha \sqrt{E})$ , can be seen, indicating trap-limited hopping conduction. The curve for the 0.1 w% provides the upper limit of experimentally reported values for the hole mobility in PE. This strengthens the hypothesis that holes are the main charge carriers in PE.

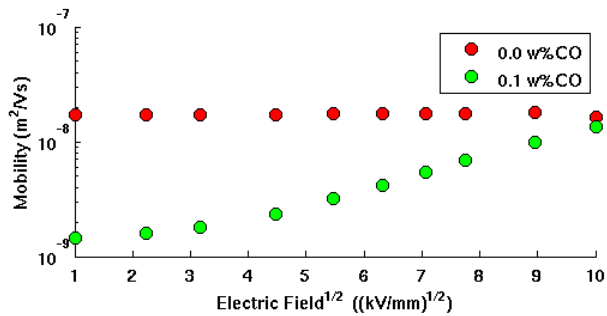


Fig. 4. Hole mobility in TRI with different concentrations of CO at 298 K (extrapolated values from high-temperature simulations to avoid finite-size effects).

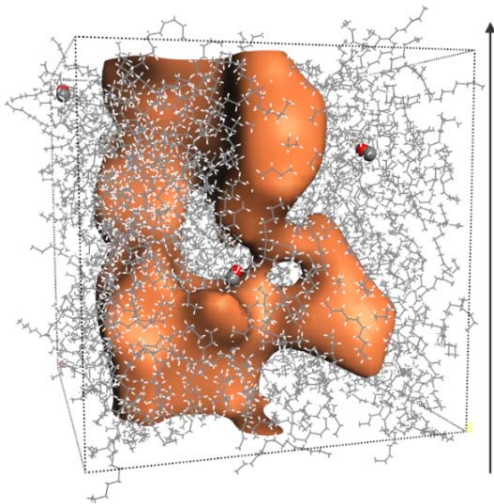


Fig. 5. The region with highest current density in the 0.1 w% system at 60 kV/mm. The arrow shows the direction of the applied electric field.

Finally, we briefly analyze the current density, in particular its spatial distribution. The current density is obtained by from the average hole velocity, which is evaluated from the occupation probabilities provided by KMC runs [26]. Note that accurate absolute values of the current density can only be obtained if the correct charge density is used in the KMC simulations. In the present study, with only one charge carrier per simulation box, only relative values are obtained. In Fig. 5 the regions with highest current density are shown for the system with 0.1 w% CO at 298K and at 60 kV/mm. The isovalue of the surface is chosen such that the charge percolating paths can be visualized. Note that all carbonyl groups are located outside the volume with the high current density. The lowest and highest values of the local current density differ by ca 3 orders of magnitude.

#### IV. CONCLUSIONS

In conclusion, we used a multiscale computational scheme to study hole transport in pristine and oxidized TRI. At moderate concentrations of oxidized states, modeled by carbonyl groups, the mobility in the system decreases by an order of magnitude. The field-dependence of the mobility

shows a typical Poole-Frenkel relation. At the highest carbonyl concentration the mobility is extremely low, indicating that ionic conduction will dominate in the system. The expected transition to a situation where charges percolate through carbonyl groups did not occur in this model. A more accurate oxidation model with random positioning of the carbonyl groups might allow observing this effect. TRI was studied since it can be seen as a model for the amorphous phase of PE. For TRI with a low trap concentration the mobility is in the same order of magnitude as the highest reported values for PE, which strengthens the hypothesis that holes dominate transport in PE. The 3D current density was analyzed for an exemplary system with low carbonyl concentration. A region with high current density could be observed with carbonyl groups located outside this volume. Finally, we conclude that the approach used here, combined with a more accurate morphology, will allow to study the mobility in PE in great detail.

#### ACKNOWLEDGEMENT

Carl Poelking is acknowledged for valuable input on computational details.

#### REFERENCES

- [1] R. M. E. A. C. Ashcraft, and R. G. Shaw, "Laboratory Studies of Treeing in Solid Dielectrics and Voltage Stabilization of Polyethylene," *IEEE Intern. Sympos. Electr. Insul.*, p. 6, 1976.
- [2] H. M. Banford, R. A. Fouracre, A. Fautitano, A. Buttafava, and F. Martinotti, "The influence of chemical structure on the dielectric behavior of polypropylene," *IEEE Trans. Diel. El. Ins.*, vol. 3, pp. 594-598, 1996.
- [3] T. Mizutani, T. Tsukahara, and M. Ieda, "The effects of oxidation on the electrical conduction of polyethylene," *J. Phys. D: Appl. Phys.*, vol. 13, p. 1673, 1980.
- [4] N. Hozumi, T. Takeda, H. Suzuki, and T. Okamoto, "Space charge behavior in XLPE cable insulation under 0.2-1.2 MV/cm dc fields," *IEEE Trans. Diel. El. Ins.*, vol. 5, pp. 82-90, 1998.
- [5] K. Ogawa, T. Suzuki, S. Katakai, M. Kanaoka, and Y. Sekii, "DC characteristics of cable insulating materials (part 1)," in *Proc. 21<sup>st</sup> Symp. Elec. Ins. Mat.*, 1988, pp. 275-278.
- [6] J. Jonsson and C. Törnkvist, "Space charge injection as a function of carbonyl group content in polyolefins," in *Nordic Ins. Symp.*, Bergen, Norway, 1996, pp. 217-224.
- [7] B. Vissouvanadin, *et al.*, "Impact of concentration gradient of polarizable species on the electric field distribution in polymeric insulating material for HVDC cable," *IEEE Trans. Diel. El. Ins.*, vol. 18, pp. 833-839, 2011.
- [8] S. Serra, G. C. Montanari, and L. A. Dissado, "Charge density stabilised local electron spin pair states in insulating polymers," *J. Appl. Phys.*, vol. 116, p. 224901, 2014.
- [9] T. J. Lewis and J. P. Llewellyn, "Electrical conduction in polyethylene: The role of positive charge and the formation of positive packets," *J. Appl. Phys.*, vol. 113, pp. 223705-223705-12, 2013.
- [10] M. Meunier, N. Quirke, and A. Aslanides, "Molecular modeling of electron traps in polymer insulators: Chemical defects and impurities," *J. Chem. Phys.*, vol. 115, pp. 2876-2881, 2001.

- [11] A. Huzayyin, S. Boggs, and R. Ramprasad, "Density functional analysis of chemical impurities in dielectric polyethylene," *IEEE Trans. Diel. El. Ins.*, vol. 17, pp. 926-930, 2010.
- [12] M. Unge, T. Christen, and C. Törnkvist, "Space charges and deep traps in polyethylene – ab initio simulations of chemical impurities and defects," *IEEE Int. Conf. on Sol. Diel.*, Bologna, Italy, 2013, pp. 935-939.
- [13] M. C. Righi, *et al.*, "Surface States and Negative Electron Affinity in Polyethylene," *Phys. Rev. Lett.*, vol. 87, p. 076802, 2001.
- [14] Y. Wang, D. MacKernan, D. Cubero, D. F. Coker, and N. Quirke, "Single electron states in polyethylene," *J. Chem. Phys.*, vol. 140, pp. -, 2014.
- [15] M. Unge, T. Christen, and C. Törnkvist, "Electronic structure of polyethylene - Crystalline and amorphous phases of pure polyethylene and their interfaces," *Rep. Conf. Elect. Insul. Diel. Phen.*, Montreal, Canada, 2012, pp. 525-530.
- [16] D. Cubero, N. Quirke, and D. F. Coker, "Electronic transport in disordered n-alkanes: From fluid methane to amorphous polyethylene," *J. Chem. Phys.*, vol. 119, pp. 2669-2679, 2003.
- [17] D. Cubero and N. Quirke, "Computer simulations of localized small polarons in amorphous polyethylene," *J. Chem. Phys.*, vol. 120, pp. 7772-7778, 2004.
- [18] J. A. Anta, G. Marcelli, M. Meunier, and N. Quirke, "Models of electron trapping and transport in polyethylene: Current – voltage characteristics," *J. Appl. Phys.*, vol. 92, pp. 1002-1008, 2002.
- [19] U. Gedde and A. Mattozzi, "Polyethylene Morphology," in *Long Term Properties of Polyolefins*. vol. 169, A.-C. Albertsson, Ed., ed: Springer Berlin Heidelberg, 2004, pp. 29-74.
- [20] O. L. Hestad, P. O. Astrand, and L. E. Lundgaard, "N-tridecane as a model system for polyethylene: comparison of pre-breakdown phenomena in liquid and solid phase stressed by a fast transient," *IEEE Trans. Diel. El. Ins.*, vol. 18, pp. 1929-1946, 2011.
- [21] S. L. Roy, G. Teyssedre, C. Laurent, G. C. Montanari, and F. Palmieri, "Description of charge transport in polyethylene using a fluid model with a constant mobility: fitting model and experiments," *J. Phys. D: Appl. Phys.*, vol. 39, p. 1427, 2006.
- [22] G. Chen, T. Y. G. Tay, A. E. Davies, Y. Tanaka, and T. Takada, "Electrodes and charge injection in low-density polyethylene using the pulsed electroacoustic technique," *IEEE Trans. Diel. El. Ins.*, vol. 8, pp. 867-873, 2001.
- [23] S. Serra, E. Tosatti, S. Iarlori, S. Scandolo, and G. Santoro, "Interchain electron states in polyethylene," *Phys. Rev. B*, vol. 62, pp. 4389-4393, 2000.
- [24] T. Tanaka and J. H. Calderwood, "Carrier Mobility in Polyethylene," *The Trans. of the Inst. of Elect. Engine. of Japan.A*, vol. 93, pp. 473-480, 1973.
- [25] T. Mizutani, "Behavior of Charge Carriers in Organic Insulating Materials," *Rep. Conf. Elect. Insul. Diel. Phen.*, 2006, pp. 1-10.
- [26] V. Rühle, *et al.*, "Microscopic Simulations of Charge Transport in Disordered Organic Semiconductors," *J. Chem. Theory and Computation*, pp. 3335-3345, 2011.
- [27] P. Kordt, *et al.*, "Modeling of Organic Light Emitting Diodes: From Molecular to Device Properties," *Adv. Funct. Mat.*, vol. 25, pp. 1955-1971, 2015.
- [28] P. J. Flory, *Statistical mechanics of chain molecules*. New York: Interscience, 1969.
- [29] G. R. Hutchison, M. A. Ratner, and T. J. Marks, "Hopping Transport in Conductive Heterocyclic Oligomers: Reorganization Energies and Substituent Effects," *J. Amer. Chem. Soc.*, vol. 127, pp. 2339-2350, 2005.
- [30] R. A. Marcus, "Electron transfer reactions in chemistry. Theory and experiment," *Rev. Mod. Phys.*, vol. 65, pp. 599-610, 1993.
- [31] M. Valiev, *et al.*, "NWChem: A comprehensive and scalable open-source solution for large scale molecular simulations," *Comp. Phys. Comm.*, vol. 181, pp. 1477-1489, 2010.
- [32] B. Baumeier, J. Kirkpatrick, and D. Andrienko, "Density-functional based determination of intermolecular charge transfer properties for large-scale morphologies," *Phys. Chem. Chem. Phys.*, vol. 12, pp. 11103-11113, 2010.
- [33] A. Lukyanov and D. Andrienko, "Extracting nondispersive charge carrier mobilities of organic semiconductors from simulations of small systems," *Phys. Rev. B*, vol. 82, p. 193202, 2010.